Exploring Nano-sulfide Enhancements on the Optical, Structural and Thermal Properties of Polymeric Nanocomposites

Jamal Q. M. Almarashi[1] · M. H. Abdel-Kader[1,2]

Abstract

Copper sulfide (CuS) nanoparticles were synthesized by solid-state reaction method under the flow of nitrogen. Polyvinyl alcohol/polyethylene glycol/copper sulfide (PVA/PEG:CuS) nanocomposite films with different concentrations of copper sulfide nanoparticles (1%, 3%, 5%) were prepared using casting technique. Structural and morphological properties of the prepared nano samples were investigated using X-ray diffraction data (XRD), transmission electron microscope and energy dispersive spectrometry techniques. The formation of nanocomposite films was confirmed by both XRD and fourier transform infrared techniques. Calculated and measured nano material particle size is almost similar. The characteristic peaks of nanocomposite films were found to be shifted towards higher wavenumber. The thermal stability behavior of row (PVA/PEG) blends and (PVA/PEG:CuS) nanocomposite films was examined using the thermogravimetric analysis technique. Samples doped with 5% CuS concentration revealed the highest thermal stability. The optical properties of undoped and nanocomposite films have been discussed in details using UV–Vis spectrophotometer. The optical transmittance revealed an apparent decrease (more than 40% for films doped 5% CuS). Different optical constants and dispersion parameters were discussed in detail and proved to be directly affected by nano doping concentrations. The optical energy gap values of polymer films decreased from 5.3 to 3.3 eV with the CuS nanoparticles incorporation. The study of the PVA/PEG nanocomposite films based on CuS nanoparticles has not been previously discussed. Therefore, this study is considered a new piece of work.

Keywords Nano CuS · Blend · Nanocomposite · Structural · Thermal · Optical

1 Introduction

Polymers drew the attention of many workers in modern industries included device design and fabrication because of their inveterate characteristics when blended together compared to individual ones [1]. It has been reported earlier, the properties of new polymeric materials can be manipulated to the desired limit through doping with either ordinary metal fillers or nanoparticles. Both polyvinyl alcohol (PVA) and polyethylene glycol (PEG) polymers are water-soluble and have a wide range of applications because of their stability and easy processibility [2]. The addition of other plasticizers of higher transparency and lower molecular weight such

as PEG to a polymer matrix took great importance between researchers because of the simple manipulation process for the development of perfectly promising miscible polymer blends without any chemical treatments. The process promotes physical properties such as plasticity, permeability, elasticity and flexibility besides other thermal, optical and electrical properties of the resulting polymeric material. This is apparent through the variation in the internal structural composition along the hydrocarbon chains by newly formed hydrogen bonds. Comparing with other polymeric materials, PVA–PEG blends proved their applicable effectiveness in the field of research and industry such as an enhancement in the crosslinking characteristics and a decrease in the melting point without any external additives and under the effect of different electron beam irradiation doses [3]. Adding inorganic additives such as rare earth, metal salts and oxides to (PVA/PEG) polymeric blends exhibit major modifications in their intermolecular structures. An increase in the optical conductivity of the blends has been achieved with the content of cobalt chloride [4], Magnesium nitrate

✉ M. H. Abdel-Kader
mhkader75@yahoo.com

1 Physics Department, College of Science, Taibah University, Medina, Saudi Arabia

2 Physics Department, Faculty of Science, Ain Shams University, Cairo, Egypt

[5] and transition metal salts confirmed its effectiveness to raise the conductivity of the composite film compared to rare earth ones [6], composites based on Graphene oxide (PVA/PEG:GO) revealed high efficiency in water purification [7] and enhanced the dielectric behavior of PVA/PEG/GO composites [8]. The optical properties of (PVA:PEG/MnCl$_2$) composites increased with manganese chloride [9] and natural additives [10]. Results showed that, the properties of these materials could be easily adjusted to the desired purpose through changing the shape and size of the nanofillers. Nanoparticles became more attractive in various research fields due to their distinctive properties coming from the nano-scale size and the large surface area covered. It was found that, they are able to improve the physical and structural characteristics of the host polymeric materials better than conventional metal dopants [11]. Nanostructured semiconductor sulfides have been inspected more widely because of their potential applications in different technological fields such as optoelectronics, batteries, sensors and solar energy [12, 13]. Copper sulfide (CuS), as a good semiconductor, characterized by its mercantile importance in the field of industry such as catalyst material, pigmentation material and color indicator and so on. Due to its different phases with complex structures, it attracted the interests as a good candidate for doping polymers in the form of nanofillers. Recently, many authors have been reported different morphologies for copper sulfide as nanowire, nanotube and nanovesicles [14], nano-rods or nanoparticles with a very good uniform spherical shape [15, 16]. The preparation method of copper sulfide in different forms has been discussed earlier by many techniques including chemical deposition, electro-deposition at room temperature and evaporation under vacuum [17, 18]. The influences of different nanoparticles added to (PVA/PEG) blends for specific deep intense modifications and compositional improvements to produce polymeric materials with a high standard level of durability against environmental variations for industrial applications have been reported earlier. Oxide nanoparticles played an essential role in the synthesizing process of nanocomposite films. Tin oxide (SnO$_2$) nanofibers increased the dielectric constant of the resulting nanofiber films [19], Graphene oxide nanoparticles positively affected the nanocomposite films electrical conductivity [20] and improved its mechanical properties [21], magnesium oxide (MgO) nanoparticles enhanced the optical properties of the (PVA–PEG–MgO) films [22], its AC conductivity [23] and its biomedical applications [24], TiO$_2$ nanoparticles increased the ionic conductivity and the humidity sensing behavior [25, 26], zinc oxide improved the optical properties of (PVA–PEG–ZnO) nanocomposites [27]. Several authors investigated the accomplishments performed in the structural, optical, thermal, dielectric properties and antibacterial behavior as well of (PVA–PEG) polymeric blends due to the

effect of silver nanoparticles [28–31]. Only very few works in the literature have been done to investigate the effect of copper sulfide nanoparticles on polymeric materials [15, 18, 32–34] and nothing referred to the effect of CuS nanoparticles on PVA/PEG blends. From the survey in the literature authors, it is confirmed that, to the best of our knowledge the study of the PVA/PEG nanocomposite films based on CuS nanoparticles has not been previously discussed. Therefore, the study of the improvements produced to the PVA/PEG blends under the influence of CuS nanoparticles is a new piece of work.

In this work, PVA/PEG/CuS nanocomposite films were performed by a simple casting technique. An extensive studies were done to represent a detailed image for the variations occurred to the optical, thermal and structural characterizations of the nanocomposite films using the UV–Vis spectrophotometer technique, Thermogravimetric analysis (TGA) and X-ray diffraction technique besides Fourier transform infrared (FTIR) spectroscopy as well, respectively. The modifications and enhancements of the optical, structural and thermal characteristics suggest that these (PVA/PEG: CuS) nanocomposite films can be used in various technological and industrial fields such as optoelectronic devices and solar cells.

2 Experimental

CuS nanoparticles were synthesized by mixing, grounding and heating a Copper Acetate and Thiourea with stoichiometric ratio 1:2 under flows of N$_2$ in an electric oven at 300 °C (optimum temperature) [35]. (PVA/PEG) row blends were prepared by casting method, dissolving 70% of polyvinyl alcohol (PVA) (degree of hydrolysis = 99%, molecular weight = 27,000 g/mol) and 30% Polyethylene glycol (PEG) (powder, molecular weight = 4000 g/mol) in distilled water under stirring at 70 °C until the solution became very clear [36]. For (PVA/PEG: CuS) blends, the above similar mixture was then obeyed for ultrasonic at 60 °C for 2 h after addition of CuS nanoparticles in different ratios (1, 3 and 5%) with respect to (PVA/PEG) blend according to the following formula:

$$x(wt\%) = \frac{w_f}{w_p + w_f} \times 100$$

where w_f and w_p are the weights of CuS and (PVA/PEG) blend, respectively. The weight ratio x which used in the present work is 0.5 wt% with respect to a polymer blend. Aggregated particles were removed by using 0.2 μ syringe filters. The solution was cast into Petri dishes and placed for several days in a closed box. X-ray diffraction (Shimadzu 6000 X-ray diffractometer, λ = 1.5406 Å) was used in order

to ensure the formation of CuS nanomaterial and to investigate the homogeneity of the nanomaterial inside (PVA/PEG) polymer blend. MAUD software [37, 38] was used to confirm the formation of CuS powder. Morphology of the nanomaterial sample was identified using a transmission electron microscope (TEM, JEOL JEM-100CX). The chemical composition (Energy Dispersive Spectrometry, EDS) of CuS sample was identified by a scanning electron microscope (JEOL, JSM-5910LV). Thermogravimetric analysis (TGA) was performed using the Perkin Elmer TGA instrument with heating rate = 10 °C/min under ambient atmosphere air (35–500 °C). The different optical parameters for different blends were determined by UV–Vis spectrophotometer (Model Tomos UV-1800) spectrophotometer technique. FTIR spectroscopy (Bruker Tensor 27 FTIR Spectrometer) was used in the range of 400–4000 cm^{-1} to confirm the existence of CuS nanomaterial inside (PVA/PEG) blends.

3 Results and Discussion

3.1 Structural Investigation Analysis

Figure 1a, shows the Rietveld refinement fitting for the XRD data of CuS using MAUD software. The diffraction pattern has a single phase with a hexagonal structure (P63/m) [39]. The experimental XRD data (blue dot lines) are fitted with theoretical ones (in solid black lines). The difference between experimental and calculated intensities identified as a residual intensity as well and is plotted below the simulated pattern. Peak positions are marked (|) at the bottom of the pattern. The peak position at 28.01°, 29.61°, 32.26°, 33.22°, 39.16°, 48.4°, 53.01° and 59.77° are corresponding to the Miller indices (hkl) planes of the (101), (102), (103), (006), (105), (110), (108) and (116) planes of the hexagonal structure (P63/m), respectively. The crystallite size of the sample was 10 nm which determined using Scherrer formula:
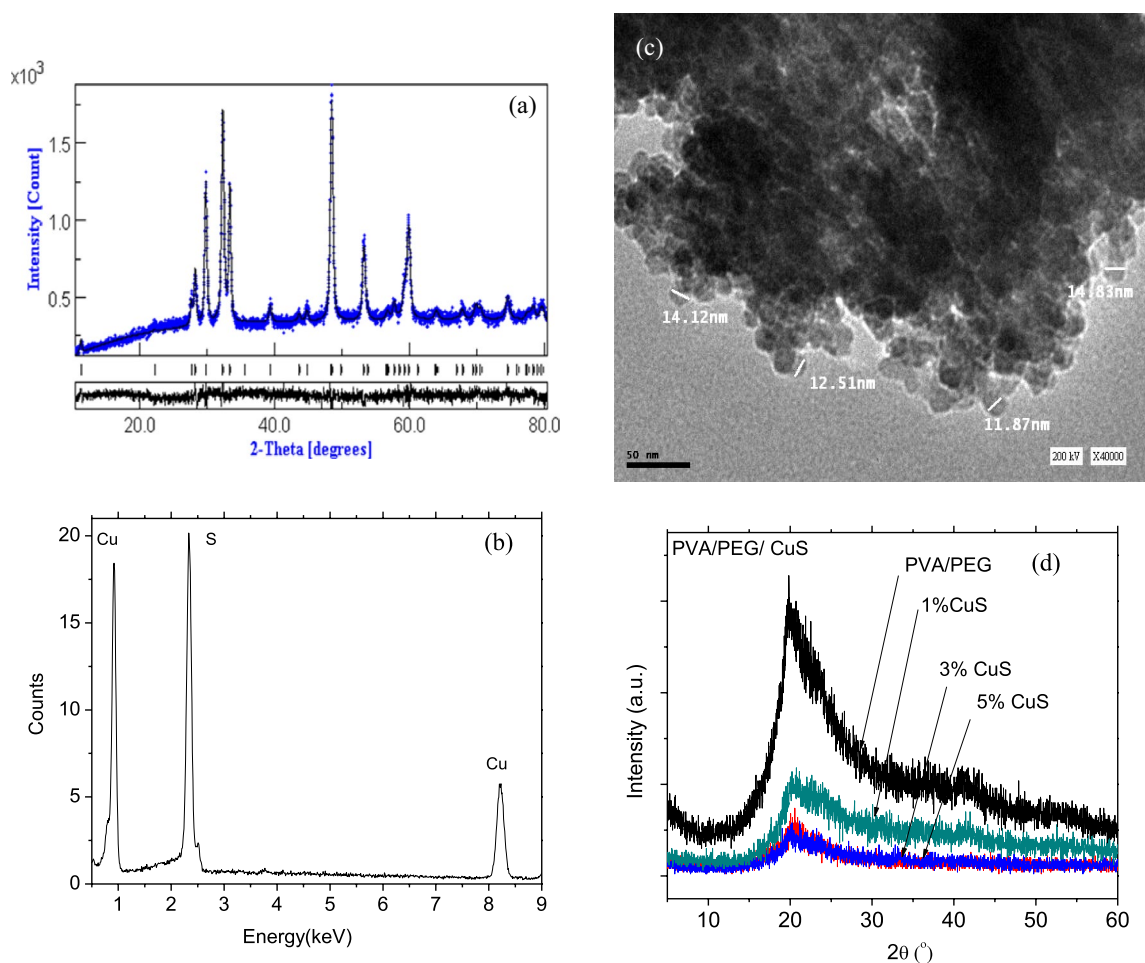

Fig. 1 **a** Reitveld refinement of CuS, **b** EDX for CuS, **c** TEM image for CuS and **d** XRD diffractions for pure and CuS doped (PVA/PEG) blends

$$L = \frac{0.9\lambda}{\beta \cos\theta}$$

where λ and β are the wavelength and half of maximal intensity, respectively.

TEM micrograph of CuS nanoparticles is revealed in Fig. 1c; nanoparticles were well characterized with average size around 12 nm which is a bit larger than the result obtained from XRD data. EDS image for CuS is revealed in Fig. 1b; where the sample contained only Cu and S elements. Inspecting Fig. 1d, the diffraction patterns of (PVA/PEG) and (PVA/PEG:CuS) nanocomposite samples were nearly identical with the main diffraction peak observed at 2θ = 21°, corresponding to partial crystallinity structure [40]. No diffraction peaks corresponding to CuS nanoparticles, manifesting complete homogeneous dissolution in (PVA/PEG) polymeric matrix.

FTIR spectroscopy is an effective and a sensitive tool that can be used to confirm the formation and interaction of the functional groups, as well as the resulting change in material arrangement. Figure 2 displays the FTIR measurement spectra of the pure PVA/PEG and the dopeded blend using different concentrations of CuS (1%, 3% and 5%) in the wavenumber range of 4000–500 cm^{-1}. The FTIR spectra revealed different peaks associated with the pure and CuS doped PVA/PEG blends. The FTIR spectra for all PVA/PEG and PVA/PEG/CuS blends exhibit a broad peak located around 3500 cm^{-1} which can be related to the stretching vibration OH^{-} groups [41], with a slight shift in peak position that can be attributed to the H-bond formation [42]. There is a sharp peak can be observed at 2900 cm^{-1} that can be attributed to the stretching CH$_2$ group [43]. The
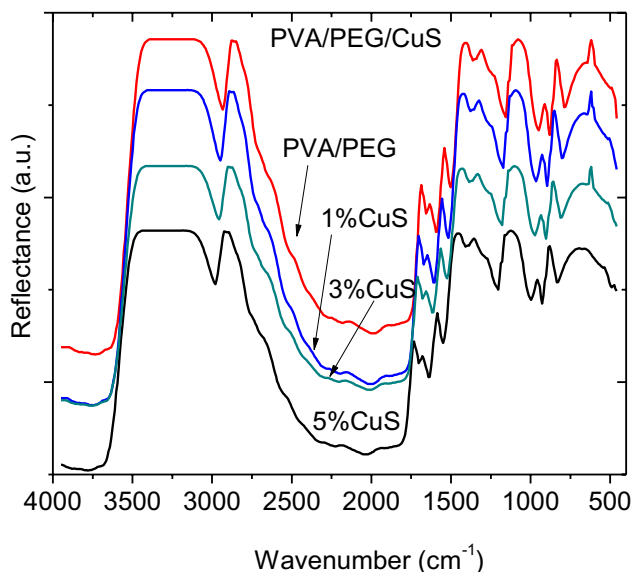
peak at around 1650 cm^{-1} is indicating the deformation of vinyl alcohol [44]. The presence of stretching C =O carbonyl group of the acetate group was confirmed from the peaks at 1732 cm^{-1} and 1569 cm^{-1} [45]. The peaks around 1450 cm^{-1}, 1375 cm^{-1} and 1050 cm^{-1} associated with symmetry CH$_2$ bond, stretching vibrations related to mixed CH^{-}and OH^{-} bending modes, and the C–C stretching mode related to the regular repetition of the trans-configuration of the zigzag chain in a crystalline region, respectively [46]. The obtained peak at 925 cm^{-1} is indicating the syndiotactic structure with strong vibration [46]. In addition, the observed peak positions shift is indicating the presence of doped material.

3.2 Thermal Analysis

Figure 3 reveals Thermogravimetric analysis (TGA) of (PVA/PEG) and (PVA/PEG: CuS) nanocomposite polymers from room temperature to 500 °C with a heating rate of 10 °C/min. All nanocomposite polymer films showed one degradation stage. This degradation stage had a peak at 92 °C for (PVA/PEG) which changed nonlinearly with change in CuS content within the (PVA/PEG) blend matrix. The weight loss was attributed to the evaporation of the physically weak and chemically strong bound of H$_2$O from the polymer matrix [47]. One can notice that 5% CuS doped (PVA/PEG) nanocomposite films reveal the highest thermal stability compared to others. The enhancement in the thermal stability upon doping of (PVA/PEG) with CuS nanoparticles at certain doping ratios may due to the interaction of nanomaterials with hydroxyl groups of the polymer (PVA/PEG) [48]. A similar observation was noticed in insertion of the CdS or ZnS in PMMA polymer matrix [49]. Moreover, the thermal degradation stability of PVA was increased as it was doped with 8–12% of cellulose nanocrystals [50]. Furthermore, the other fluctuations appeared in DTG with temperature (Fig. 3b) was due to degradation of the side chain (O–H) and the cleavage of C–C backbone (carbonation) of (PVA/PEG) polymer blend [50].

3.3 UV-Spectroscopy Analysis

The study of the characteristic absorption band edge in the UV region is a very important method for understanding the variations in the internal band structure through investigating optically induced electronic transitions within polymeric materials. The absorption and transmission spectra for pure PVA/PEG films and nanocomposite ones are shown in Fig. 4. It is clear from the figures that, an absorption band with a low rise peak centered at 320 nm in the UV region is observed for pure and composite films. These results are in similar agreement with those represented earlier [36, 51, 52]. The little variation in the
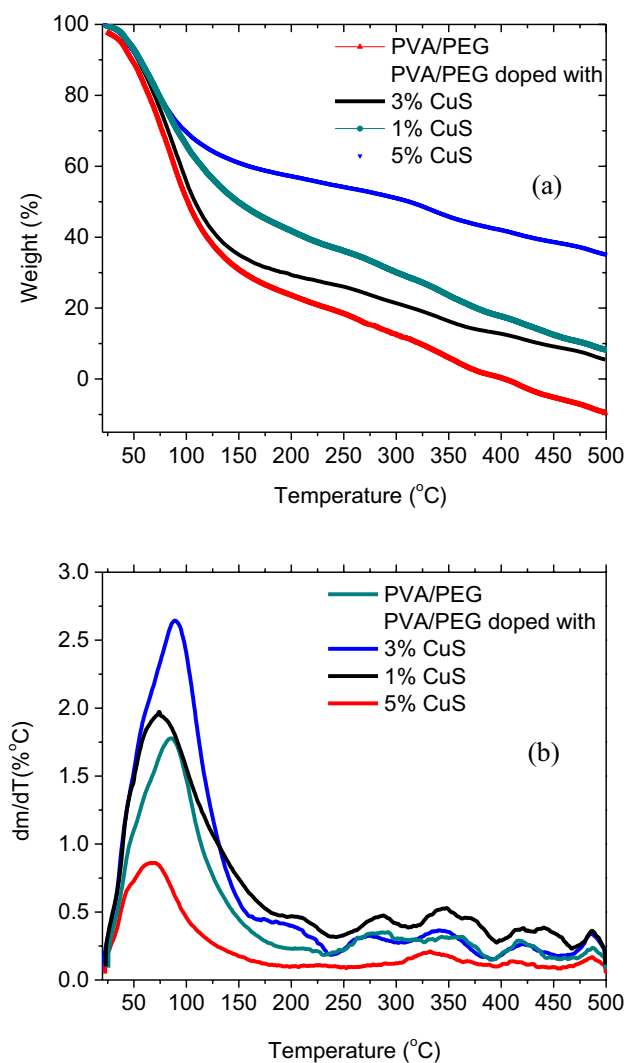
Fig. 2 IR for pure and CuS doped (PVA/PEG) blends

Fig. 3 Thermogravimetric curves for pure and CuS doped (PVA/PEG) blends. **a** TGA (Thermogravimetric analysis) and **b** DTG (Differential Thermogravimetric)

Fig. 4 UV–Visible **a** absorbance and **b** transmittance spectra of pure and CuS doped (PVA/PEG) blends

absorption peak position could be returned to the ratios of different concentrations mixed together from both polymers besides, the dopant material used. Others referred this variation to the different molecular weights of polymers used [53]. The appearance of this absorption band is attributed to the transitions of the unshared electron pairs upon unsaturated bonds C=O and C=O along with the blend structure [36, 54]. No absorption bands can be noticed in the visible region indicating high transparency behavior for all samples. An enhancement in the measured absorption spectra along the whole spectral range for the films doped with CuS nanoparticles has been observed. This enhancement increases with the dopant concentration. The increase in the absorption behavior with CuS nanoparticles concentrations can be considered as evidence for the mutual interaction between nanoparticles
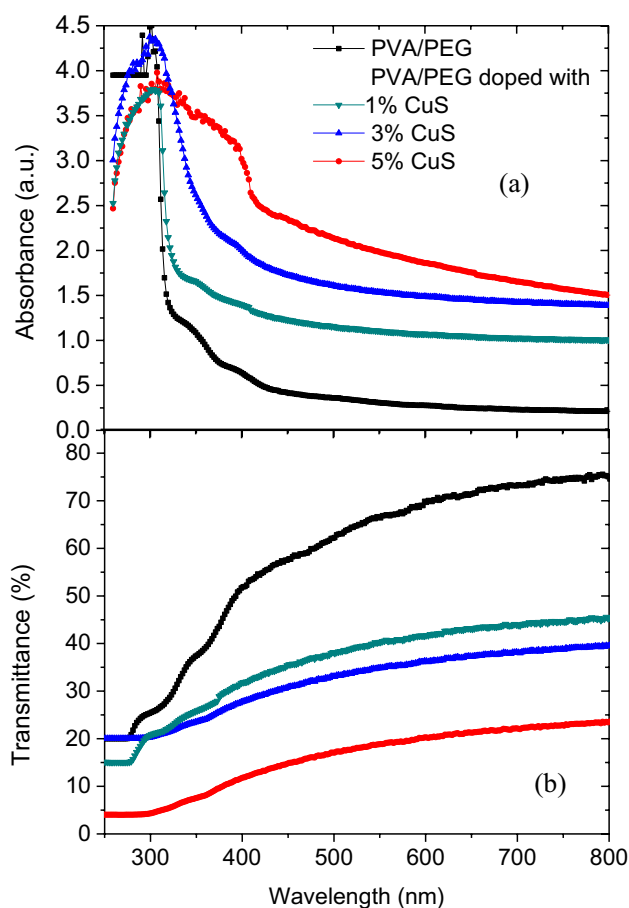
and the polymer matrix [55, 56]. This can be interpreted on the basis of the formation of new intermolecular bonds between $[Cu^{2+}]$ cations and $[OH^-]$ anions along the whole polymer backbone chain giving rise to a change due to new defects $Cu(OH)_2$. These are responsible for stresses that occur within internal structure. The decrease in the absorption spectra within the range (320–800 nm) for all samples with the increase in the wavelength can be returned to the change (decrease) in the energy of the incident light [57, 58]. The increase in the absorbance values for nanocomposite films with increasing nanoparticle concentrations from 1 to 5% corresponds to a decrease in the transmittance values as shown in Fig. 4b. Only the scattering process is the principal factor that affects light transmission. As the density of the added nanoparticles increases with concentration, the probability of light scattering at the grain and defects boundaries rises and hence transmittance decreases. The decrease in the transmittance as well as the increase in the optical absorption edge width with doping concentrations reflects the amorphous nature of the samples [59]. The extinction coefficient (*k*)

and refractive index (n) are the most important optical parameters. In fact, they are generally called optical constants. k describes the absorption behavior of the material when exposed to light and it measures the fraction of the squandered energy from the incident beam of photons per unit length of the medium [60]. Refractive index n is an optical parameter that describes the polarizability of molecules under the effect of the electromagnetic field of the incident beam of photons [61–63]. The relation between the refractive index of an isotropic medium, the number of molecules per unit volume and molecules polarizability can be understood well from the famous Lorentz–Lorenz relation [64].

n and k are represented by the following equations [65, 66]:

$$n = \frac{1+R}{1-R} + \sqrt{\frac{4R}{(1-R)^2} - k^2} \tag{1}$$

where k is:

$$k = \frac{\lambda \alpha}{2\pi} \tag{2}$$

and α is:

$$\alpha(\lambda) = \left(\frac{2.303}{d}\right)A \tag{3}$$

where R, α, λ, A and d are the reflectance, the absorption coefficient, the wavelength, the absorbance and the film thickness. The absorption coefficient α is the parameter that evaluates the absorption process of light by the medium. It is the energy absorbed per unit length of the medium in unit time [67]. According to Eq. 2, a consistency in behavior and peak position is expected between the optical spectra of the extinction coefficient and these of the absorption ones for both undoped and nanocomposite films (figure not shown). This can be explained as: the increase in the amount of doping increases the fraction absorbed of the incident photons due to the scattering process [68]. Figure 5 represents the refractive index spectra for both undoped and nanocomposite films. The spectra exhibit faint dispersion peaks in the high-energy region while taking a plateau shape in the low one. The peak for 5% CuS doping looks clearer a little bit compared to others which enhances the effect of doping. It is clear from Fig. 5 that the refractive index spectra increase with doping concentration and the appearance of the dispersion peaks in the high energy region reflects the polarization effect that occurred to the molecules of the film due to the existence of the incident light electromagnetic field and different concentrations of nanoparticles [69, 70]. In other words, increases the dopant concentration enhances the polarization phenomena because of the enhancement
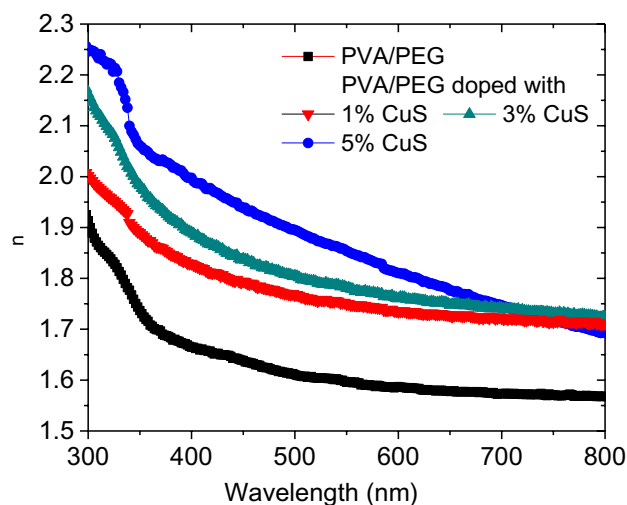

Fig. 5 Wavelength dependent of refractive index for pure and CuS doped (PVA/PEG) blends

in the intermolecular structure by increasing the material density due to the increase in the number of bonds formed between CuS nanoparticles and OH groups along the polymer backbone chain. In other words, these defect bonds are responsible for stressing (decrease interatomic spacings) nanocomposite films showing a rise in its density. In the visible region, the molecules are characterized by its own inertia and are not affected by the incident electromagnetic field.

The detailed analysis of the absorption process is very necessary for providing information about the optical band gap internal structure and the investigation of possible electronic transitions. The optical band gap can be described as the energy gap between the valance and conduction bands. The direct optical energy gap E_g values can be extracted based on the well-known famous Tauc equation [39, 71]:

$$\alpha h\upsilon = A\left(h\upsilon - E_g\right)^n \tag{4}$$

where h,υ, A and n are Planck's constant, incident light frequency, is a constant and n is a parameter takes values depend on the type of transition; becomes 1/2 or 2 for direct allowed or indirect allowed band gap semiconductors, respectively [72, 73]. The graphical relationship between $(\alpha h\upsilon)^2$ and the photon energy ($h\upsilon$) (direct allowed transition) for undoped PVA/PEG and doped PVA/PEG:CuS nanocomposite films is shown in Fig. 6. One can notice that, all nanocomposite films show similar absorption edge attitude with a shift towards the low energy side by increasing nano-dopant concentration. E_g values are considered equal to $h\upsilon$ when $(\alpha h\upsilon)^2 = 0$, so E_g values can be extracted from the graph by extrapolating the linear part to the x-axis. Table 1 represents the extracted values of E_g. It is clear that, increasing
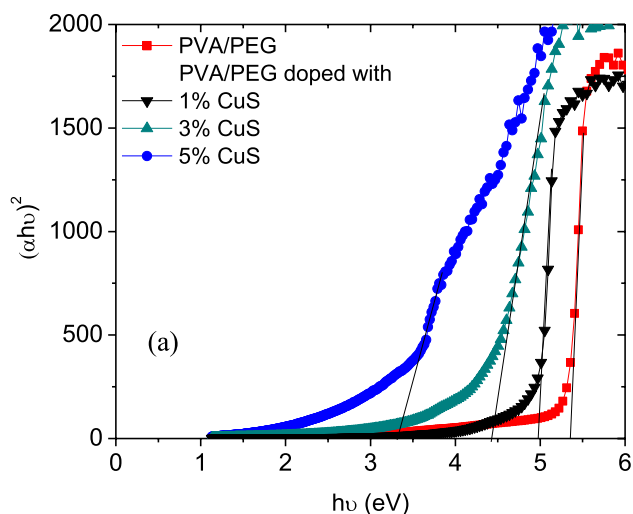
Fig. 6 Energy dependence of $(\alpha h \upsilon)^2$ for pure and CuS doped (PVA/PEG) blends

Table 1 Energy gaps and dispersions parameters for row (PVA/PEG) and (PVA/PEG:CuS) blends

	Gap energy E_g (eV)	E_o (eV)	E_d (eV)
PVA/PEG	5.3	6.9	9.9
PVA/PEG doped with			
1% CuS	4.9	6.1	12
3% CuS	4.4	5.6	13.7
5% CuS	3.3	5.3	14

the nano-dopant concentrations in the sequence 1%, 3% and 5% changes the energy gap values from 5.3 eV for undoped PVA/PEG samples to 4.9, 4.3 and 3.3 eV respectively. This behavior in the E_g values can be interpreted as: the rise in the nano-dopant concentration increases the degree of disordering of the polymer matrix by introducing some defects (bonds formed between CuS nanoparticles and OH groups) to the structure. These defects are responsible for the production of new localized states within band gap region, similar results to ours have been represented elsewhere [1, 2, 6].

The effective single-oscillator approximation model of Wemple and DiDomenico discussed in detail the dispersion data for more than one hundred materials (crystalline and amorphous) [74, 75]. They found that the following relation [76–78] could describe the optical data related to the refractive index n (at energy values less than that of the absorption edge), with a very good approximation:

$$n^2(h\upsilon) = 1 + \frac{E_o E_d}{E_o^2 - (h)^2} \qquad (5)$$

where the dispersion parameters E_o and E_d are the single-oscillator energy and the dispersion energy, respectively. E_d is also called the oscillator strength because it describes the strength of interband optical transitions and it depends on the effective number of valence electrons. Experimentally, E_d doesn't depend on either the E_g value or the valence electrons volume density [79]. E_o is also representing the mean energy of the electronic transitions between the valance band and the conduction band. It is empirically related to the E_g value as ($E_o \approx 1.3 E_g$) which is in a good agreement with others [74–78]. The values of the dispersion parameters E_d and E_o can be obtained by plotting the relation between $(n^2 - 1)^{-1}$ and $(h\upsilon)^2$ and fitting straight lines as shown in Fig. 7. From the graph, $\left(slope = \frac{-1}{E_o E_d}\right)$ and (Interception point on the vertical axis $= \frac{E_o}{E_d}$). The calculated values of E_o and E_d are tabulated in Table 1. As E_o and E_g are closely related to the previously mentioned empirical formula, E_o represents a clear image for the alterations that occur within the band gap region. Therefore, the decrease in E_o values was expected and proves the existence of a high degree of disordering within the structure due to the presence of defects as localized states under the influence of different concentrations.

The decrease in E_o values is consistent with the decrease in E_g values. Other groups represented results similar to ours [80, 81]. As E_d correlated to the strength of the optical transitions and depends on the number of valence electrons, the increase in E_d values with the doping concentration rise means, an excess number of valence electrons will be available. This confirms the explanation discussed before concerning the formation of new bonds along the polymer structure increasing the number of new defects within it. This means,
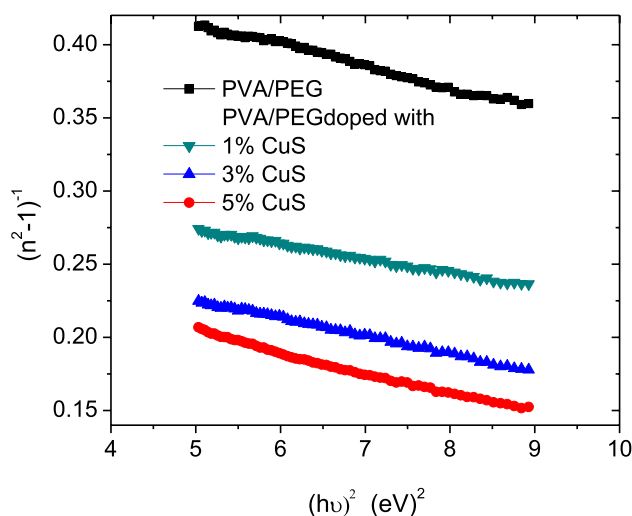

Fig. 7 Plot of $(n^2-1)^{-1}$ against $(h\upsilon)^2$ for pure and CuS doped (PVA/PEG) blends

the number of charge transfer complexes between undoped PVA/PEG samples and CuS nanoparticles increases which in turn increases the probability of electronic transitions. This behavior is in agreement with the gradual decrease in the E_g values with doping concentration as indicated in Table 1.

The optical spectroscopy study for the dielectric function is very useful for a detailed description of the material band structure. The dielectric function cannot be measured experimentally in a direct way like absorbance, reflectance and transmittance [82]. Based on the previously calculated values of the refractive index n and the extinction coefficient k, the real ($\varepsilon_r = n^2 - k^2$) and imaginary ($\varepsilon_i = 2nk$) parts of the optical dielectric constants can be investigated in this study. These parameters are in a direct relationship with the density of states inside the energy gap of the films [83–87]. ε_r refers to the dispersion in the medium while ε_i refers to the dissipation of energy of the incident electromagnetic wave by the medium. ε_r and ε_i optical spectra for undoped PVA/PEG and nanocomposite films at different concentrations are shown in Fig. 8. It is obvious from the figure that, the optical

behavior for ε_r spectra shows a gradual decrease with the wavelength beyond the absorption edge value until it reaches a nearly constant attitude. A rise in the ε_r optical spectra has been observed with the increase in the CuS nanoparticles concentration. This attitude is similar to that of the refractive index and the extinction coefficient discussed before and confirms the role of the new defect bonds formed between CuS and polymer structure. So, the increase in ε_r values with the dopant concentration can be attributed to the enhancement that occurred to the structure due to the presence of many defect bonds that are responsible for increasing the density of the material and hence its dispersion. Figure 8b shows that, the optical spectra for ε_i look have the same behavior beyond the absorption edge value for all samples. An increase in the spectral behavior with the wavelength can be observed. The increase in the ε_i values with the rise in the nanoparticles concentration reflects the dominance effect of both the extinction coefficient and the refractive index because of the direct proportionality relationship. The behavior of ε_i optical spectra is consistent with that of ε_r which indicates that the highly doped nanocomposite films dissipate much more energy of the incident electromagnetic wave when compared to the films doped with lower concentrations.

4 Conclusion

CuS nanoparticles were formed at 300 °C under the flow of nitrogen. The presence of only Cu and S elements in the resulting nano powder was confirmed with the EDS technique. The compatibility between the calculated crystallite size by Scherrer formula (~ 10 nm) and that measured experimentally (~ 12 nm) by TEM technique was maintained. The XRD diffraction spectra proved the hexagonal structure of CuS nanoparticles and the semi crystallinity nature of both undoped and nanocomposite films. The shift in the peak position of the FTIR spectra is evidence for the formation of new nanocomposite films by successful interaction between nano additives and row (PVA/PEG) blends. The TGA study showed the direct proportionality between thermal stability and the rise in the CuS nanoparticles concentrations. (PVA/PEG:CuS) nanocomposite films doped with 5% CuS revealed the highest thermal stability compared to other samples which may be due to the hydrogen bonding formation. The counter behavior between optical transmittance and absorption confirmed the mutual interaction between added nanoparticles and polymer matrix besides its amorphous nature. lower concentrations weren't possible because of negligible variations between doped nano composite samples and undoped ones when compared. The structural improvements due to new defects have been discussed in details by different optical constants and dispersion
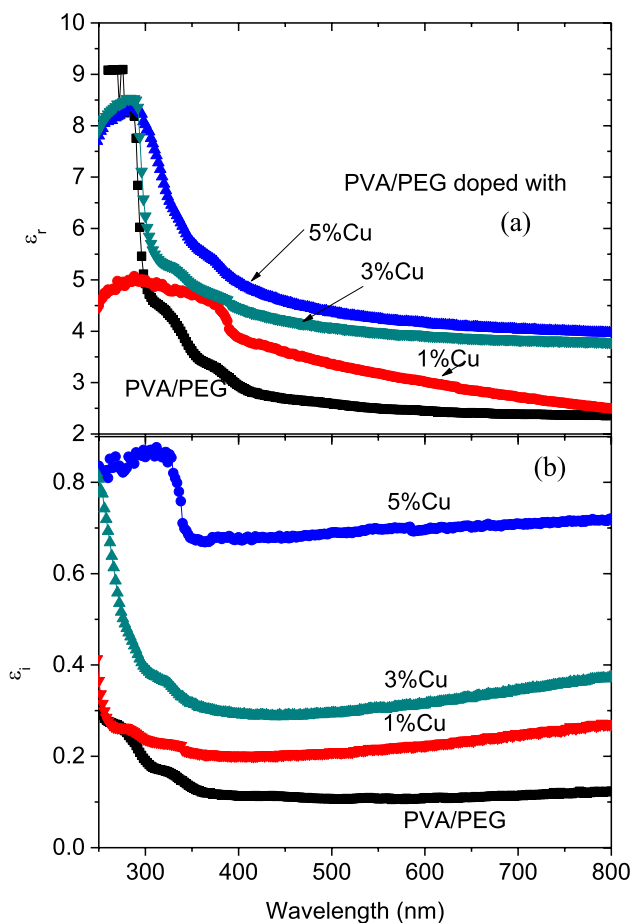

Fig. 8 wavelength dependent of **a** real part of dielectric constant and **b** dielectric loss for pure and CuS doped (PVA/PEG) blends

parameters. The polarization phenomena were found clearly affected by the doping concentration. The decrease in the energy gap (E_g) values with increasing CuS nanoparticles concentration is a promising result for future applications in the field of optoelectronic devices and solar cell fabrication.

References

1. L.Y. Jua, R.R. Karri, N.M. Mubarak, L.S. Yon, C.H. Bing, M. Khalid, P. Jagadish, E.C. Abdullah, Modeling of methylene blue adsorption using functionalized Buckypaper/Polyvinyl alcohol membrane via ant colony optimization. Environ. Pollut. **259**, 113940 (2020)

2. N.H. El Fewaty, A.M. El Sayed, R.S. Hafez, Synthesis, structural and optical properties of tin oxide nanoparticles and its CMC/PEG–PVA nanocomposite films. Composites **58**(6), 1004–1016 (2016)

3. Y. Dai, Q. Tang, Z. Zhang, C. Yu, H. Li, L. Xu, S. Zhang, Z. Zou, Enhanced mechanical, thermal, and UV-shielding properties of poly(vinyl alcohol)/metal–organic framework nanocomposites. RSC Adv. **8**, 38681–38688 (2018)

4. E.A. El-sayd, A.A. Ibrahiem, R.M. Ahmed, Effect of cobalt chloride on the optical properties of PVA/PEG blend. Arab. J. Nucl. Sci. Appl. **52**(1), 22–32 (2019)

5. D. Ravindran, P. Vickraman, XRD, Conductivity studies on PVA-PEG blend based Mg^{2+} ion conducting polymer electrolytes. Int. J. Sci. Eng. Appl. **1**(1), 72–74 (2012)

6. G. Mohammed, A. Mohamed El Sayed, Structural, morphological, optical and dielectric properties of M^{3+}/PVA/PEG SPE films (M = La, Y, Fe or Ir). Polym. Adv. Technol. **30**(3), 1–15 (2018)

7. E. Serag, A. El-Nemr, A. El-Maghraby, Synthesis of highly effective novel graphene oxide-polyethylene glycol-polyvinyl alcohol nanocomposite hydrogel for copper removal. J. Water Environ. Nanotechnol. **2**(4), 223–234 (2017)

8. K. Deshmukh, M.B. Ahamed, K.K. Sadasivuni, D. Ponnamma, R.R. Deshmukh, S.K.K. Pasha, M.A. AlMaadeed, K. Chidambaram, Graphene oxide reinforced polyvinyl alcohol/polyethylene glycol blend composites as high-performance dielectric material. J. Polym. Res. **23**(159), 1–13 (2016)

9. A. Mohammed, M.H. Suhail, M. Ghazi, Structural and optical properties for PVA-PEG-MnCl$_2$ composites. Iraq. J. Phys. **15**(32), 99–113 (2017)

10. Z. Ramdhan, M. Ali, A. Khalaf, A. Hashim, H. Hakim, Optical properties of (PVA-PEG-PF, PP) composites. Int. J. Sci. Res. **3**(10), 1725–1728 (2014)

11. M.T. Ramesan, Synthesis, characterization, and properties of new conducting polyaniline/copper sulfide nanocomposites. Polym. Eng. Sci. **54**(2), 438–445 (2014)

12. M. Ghoswami, R. Ghosh, G. Chakraborty, K. Gupta, A.K. Meikap, Optical and electrical properties of polyaniline-cadmium sulfide nanocomposite. Polym. Compos. **32**(12), 2017–2027 (2011)

13. J. Osuntokun, PA Ajibade, Structural and thermal studies of ZnS and CdS nanoparticles in polymer matrices. J. Nanomater. **13**, 1–15 (2016)

14. Q. Lu, F. Gao, D. Zhao, One-step synthesis and assembly of copper sulfide nanoparticles to nanowires, nanotubes, and nanovesicles by a simple organic amine-assisted hydrothermal process. Nano Lett. **2**(7), 725–728 (2002)

15. M.T. Ramesan, Synthesis, characterization, and conductivity studies of polypyrrole/copper sulfide nanocomposites. J. Appl. Polym. Sci. **128**(3), 1540–1546 (2013)

16. P. Bera, S. Il Seok, Nanocrystalline copper sulfide of varying morphologies and stoichiometries in a low temperature solvothermal process using a new single-source molecular precursor. Solid State Sci. **14**, 1126–1132 (2012)

17. S.S. Dhasade, J.S. Patil, J.H. Kim, S.H. Han, M.C. Rath, V.J. Fulari, Synthesis of CuS nanorods grown at room temperature by electrode position method. Mater. Chem. Phys. **137**, 353–358 (2012)

18. S.J. Abbas, M. Rani, S.K. Tripathi, Preparation and characterization of nanocomposite between poly(aniline-co-m-chloroaniline)–copper sulfide nanoparticles. Physica B **443**, 107–113 (2014)

19. M. Diantoro, L.A. Sari, T. Istirohah, A.D. Kusumawati, Nasikhudin, Sunaryono, Control of dielectric constant and anti-bacterial activity of PVA-PEG/x-SnO$_2$ nanofiber. Mater. Sci. Eng. **367**, 1–8 (2018)

20. M. Mohsen, A. Ashry, A.M. Ismail, F. El-Sayed, D.M. Abd El-Maqsoud, K.R. Mahmoud, Comparative effect of gamma irradiation on the nano-free volume and electrical properties of PVA/PEG/reduced graphene oxide nanocomposites. Arab. J. Nucl. Sci. Appl. **52**(4), 175–189 (2019)

21. F.H. Falqi, O.A. Bin-Dahman, M. Hussain, M.A. Al-Harthi, Preparation of miscible PVA/PEG blends and effect of graphene concentration on thermal, crystallization, morphological, and mechanical properties of PVA/PEG (10wt%) blend. Int. J. Polym. Sci. **2018**, 1–11 (2018)

22. B.H. Rabee, N.A. Hadi, Study the effect of nano-Mgo On the optical properties of (PVA-PEG-Mgo) nanocomposites. Int. J. Eng. Res. Technol. **3**(6), 2257–2260 (2014)

23. S. El-Gamal, A.M. El Sayed, Physical properties of the organic polymeric blend (PVA/PAM) modified with MgO nanofillers. J. Compos. Mater. **53**(20), 2831–2847 (2019)

24. R.I. Agool, J.K. Kadhim, A. Hashim, Synthesis of (PVA-PEG-PVP-MgO) nanobiomaterials and their application. Adv. Environ. Biol. **9**(27), 101 (2015)

25. M. Joshi, R.P. Singh, Cross linking polymers (PVA & PEG) with TiO$_2$ nanoparticles for humidity sensing. Sens. Trans. J. **110**(11), 105–111 (2009)

26. H. Amiri, M. Mohsennia, Impedance study of PVA/PEG/LiClO$_4$/TiO$_2$ nanocomposite solid polymer blend electrolyte. J. Mater. Sci. **28**, 4586–4592 (2017)

27. B.H. Rubee, S.A. AlHussien, Study of optical properties for (PVA-PEG-ZnO) nanocomposites. Int. J. Sci. Res. (IJSR) **5**(5), 1794–1799 (2016)

28. H.M. Mohssin, Investigation of optical properties for (PVA-PEG-Ag) polymer nanocomposites films. Int. J. Eng. Res. Technol. (IJERT) **6**(7), 164–170 (2017)

29. S.A. Nouh, K. Benthami, A.A. Alhazime, J.Q.M. Almarashi, Structural, thermal and optical behavior of laser irradiation-induced PVA–PEG–Ag nanocomposites. Radiat. Eff. Defects Solids **172**(3), 275–285 (2017)

30. S.A. Nouh, K. Benthami, M.M. Abutalib, X-ray irradiation-induced changes in (PVA–PEG–Ag) polymer nanocomposites films. Radiat. Eff. Defects Solids **171**(1), 135–145 (2016)

31. W.R. Rolim, J.C. Pieretti, D.L.S. Reno, B.A. Lima, M.H.M. Nascimento, F.N. Ambrosio, C.B. Lombello, M. Brocchi, A.C.S. de Souza, A.B. Seabra, Antimicrobial activity and cytotoxicity to tumor cells of nitric oxide donor and silver nanoparticles containing PVA/PEG films for topical applications. ACS Appl. Mater. Interfaces **11**, 6589–6604 (2019)

32. O.G.H. Abdullah, S.A. Saleem, Effect of copper sulfide nanoparticles on the optical and electrical Behavior of poly(vinyl alcohol) films. J. Electron. Mater. **45**, 5910–5920 (2016)

33. M.T. Ramesan, Fabrication and characterization of conducting nanomaterials composed of copper sulfide and polyindole. Polym. Compos. **33**(12), 2169–2176 (2012)

34. H. Jin, Y. Hou, A. Tang, X. Meng, F.T. Feng, Photoconductive properties of MEH-PPV/CuS-nanopartile composites. Chin. Phys. Lett. **23**(3), 693–696 (2006)

35. Z.K. Heiba, M.B. Mohamed, M.H. Abdel Kader, Experimental and theoretical investigations on intermediate band in doped nano-SnS_2. Electron. Mater. **47**(5), 2945–2953 (2018)

36. M.B. Mohamed, M.H. Abdel-Kader, Effect of excess oxygen content within different nano-oxide additives on the structural and optical properties of PVA/PEG blend. Appl. Phys. A **125**(209), 1–11 (2019)

37. L. Lutterotti, Nucl. Instrum. Methods Phys. Res. B **268**, 334 (2010)

38. J. Rodríguez-Carvajal, Phys. B (Amsterdam, Neth.) **192**, 55 (1993)

39. M.B. Mohamed, M.H. Abdel-Kader, J.Q.M. Almarashi, Role of Cu/S ratio and Mg doping on modification of structural and optical characteristics of nano CuS. Int. J. Appl. Ceram. Technol. **2019**, 1–9 (2019)

40. B.G. Shetty, V. Crasta, N.B.R. Kumar, K. Rajesh, R. Bairy, P.S. Patile, Promising PVA/TiO_2, CuO filled nanocomposites for electrical and third order nonlinear optical applications. Opt. Mater. **95**, 1–10 (2019)

41. V. Balan, C. Mihai, F. Cojocaru, C. Uritu, G. Dodi, D. Botezat, I. Gardikiotis, Vibrational spectroscopy fingerprinting in medicine: from molecular to clinical practice. Materials **12**(18), 1–40 (2019)

42. F.H. Falqiet, O.A. Bin-Dahman, M. Hussain, M.A. Al-Harth, Preparation of miscible PVA/PEG blends and effect of graphene concentration on thermal, crystallization, morphological, and mechanical properties of PVA/PEG (10 wt%) blend. Int. J. Polym. Sci. **2018**, 1–11 (2018)

43. M. Pandey, G.M. Joshi, N.N. Ghosh, Electrical performance of lithium ion based polymer electrolyte with polyethylene glycol and polyvinyl alcohol network. Int. J. Polym. Mater. Polym. Biomater. **65**(15), 759–768 (2016)

44. M. Abdelaziz, Cerium (III) doping effects on optical and thermal properties of PVA films. Physica B **406**(6–7), 1300–1307 (2011)

45. K. Varatharajan, S. Govindaraj, Structural, optical and dielectric properties of PbS-PVA-PEG nanocomposite film. Sci. Adv. Mater. **4**(12), 1247–1253 (2012)

46. M. Diantoro, T. Istirohah, A. Fuad, I. Ristanti, Dielectric properties and bioactivity of $PVA/PEG/TiO_2$ fibers for capacitive based body sensor. J. Phys. **1040**, 1–9 (2018)

47. E.M. Abdelrazek, I.S. Elashmawi, A. El-khodary, A. Yassin, Structural, optical, thermal and electrical studies on PVA/PVP blends filled with lithium bromide. Curr. Appl. Phys. **10**, 607–613 (2010)

48. R. Singh, S.G. Kulkarni, Thermal and mechanical properties of nano-titanium dioxide-doped polyvinyl alcohol. Polym. Bull. **70**, 1251–1264 (2013)

49. C.H.L. Raju, J.L. Rao, B.C.V. Reddy, K.V. Brahmam, Thermal and IR studies on copper doped polyvinyl alcohol. Bull. Mater. Sci. **30**, 215–218 (2007)

50. A.M. Shehap, Thermal and spectroscopic studies of polyvinyl alcohol/sodium carboxy methyl cellulose blends. Egypt. J. Solids **31**, 75–91 (2008)

51. N.H. El Fewaty, A.M. El Sayed, R.S. Hafez, Synthesis, structural and optical properties of tin oxide nanoparticles and its CMC/PEG–PVA nanocomposite films. Compos. Polym. Sci. Ser. A **58**(6), 1004–1016 (2016)

52. K. Kannan, L.G. Prasad, L.G. Agilan, N. Muthukumarasamy, Investigations on Ag_2S/PVA-PEG polymer nanocomposites: an effectual nonlinear optical material. Optik **170**, 10–16 (2018)

53. B.H. Rabee, F.Z. Razooqi, M.H. Shinen, Investigation of optical properties for (PVA-PEG-Ag) polymer nanocomposites films. Chem. Mater. Res. **7**(4), 103–109 (2015)

54. A.M. Shehap, D.S. Akil, Structural and optical properties of TiO_2 nanoparticles/PVA for different composites thin films. Int. J. Nanoelectron. Mater. **9**, 17–36 (2016)

55. S.B. Aziz, H.M. Ahmed, A.M. Hussein, A.B. Fathulla, R.M. Wsw, R.T. Hussein, Tuning the absorption of ultraviolet spectra and optical parameters of aluminum doped PVA based solid polymer composites. J. Mater. Sci. **26**, 8022–8028 (2015)

56. G. Attia, M.F.H. Abd El-Kader, Structural, optical and thermal characterization of PVA/2HEC polyblend films. Int. J. Electrochem. Sci. **8**, 5672–5687 (2013)

57. A. Hashim, Q. Hadi, Synthesis of novel (polymer blend-ceramics) nanocomposites:structural, optical and electrical properties for humidity sensors. J. Inorg. Organometal. Polym. Mater. **28**, 1394–1401 (2018)

58. K. Ramamohan, V.B.S. Achari, A.K. Sharma, L. Xiuyang, Electrical and structural characterization of PVA/PEG polymer blend electrolyte films doped with $NaClO_4$. Ionics **21**(5), 1333–1340 (2015)

59. N. Ahlawat, S. Sanghi, A. Agarwal, S. Rani, Effect of Li_2O on structure and optical properties of lithium bismosilicate glasses. J. Alloys Compd. **480**, 516–520 (2009)

60. M.Q.A. Al-Gunaid, A.M.N. Saeed, Siddaramaiah, Effects of the electrolyte content on the electrical permittivity, thermal stability, and optical dispersion of poly(vinyl alcohol)–cesium copper oxide–lithium perchlorate nanocomposite solid-polymer electrolytes. J. Appl. Polym. Sci. **135**(8), 1–14 (2018)

61. E.A. Costner, B.K. Long, C. Navar, S. Jockusch, X. Lei, P. Zimmerman, A. Campion, N.J. Turro, C.G. Willson, Fundamental optical properties of linear and cyclic alkanes: VUV absorbance and index of refraction. J. Phys. Chem. A **113**, 9337–9347 (2009)

62. M. Born, E. Wolf, *Principles of Optics*, 2nd edn. (Pergamon Press, New York, 1964)

63. S.A. Korff, G. Breit, Optical dispersion. Rev. Mod. Phys. **4**(3), 471–503 (1932)

64. D. Beysens, P. Calmettes, Temperature dependence of the refractive indices of liquids: deviation from the Lorentz-Lorenz formula. J. Chem. Phys. **66**, 766–771 (1977)

65. A.A. Alhazime, M.B. Mohamed, M.H. Abdel-Kader, Effect of $Zn_{1-x}Mg_xS$ doping on structural, thermal and optical properties of PVA. J. Inorg. Organometal. Polym. Mater. **29**, 436–443 (2019)

66. S.A. Nouh, M.H. Abdel-kader, M.B. Mohamed, Structural and optical modifications in polyvinyl alcohol due to Cr_2O_3 nanoparticles additives concentration, and gamma irradiation. Adv. Polym. Technol. **36**(3), 1–5 (2017)

67. A.M. El Sayed, Synthesis and controlling the optical and dielectric properties of CMC/PVA blend via γ-rays irradiation. Nucl. Instrum. Methods Phys. Res. B **321**, 41–48 (2014)

68. G. Maroulis, D. Xenides, Dipole, dipole–quadrupole, and dipole–octopole polarizability of adamantane, $C_{10}H_{16}$, from refractive index measurements, depolarized collision-induced light scattering, conventional ab initio and density functional theory calculations. J. Chem. Phys. **115**(17), 7957–7967 (2001)

69. D. Sainova, A. Zen, H. Nothofer, U. Asawapirom, U. Scherf, R. Hagen, T. Bieringer, S. Kostromine, D. Neher, Photoaddressable alignment layers for fluorescent polymers in polarized electroluminescence devices. Adv. Funct. Mater. **12**(1), 49–57 (2002)

70. I. Simonsen, Optics of surface disordered systems. A random walk through rough surface scattering phenomena. Eur. Phys. J. Spec. Top. **181**, 1–103 (2010)

71. M.B. Mohamed, M.H. Abdel-Kader, A.A. Alhazime, Structural and optical properties of doped ZnO/SiO_2 nanocomposite. Int. J. Appl. Ceram. Technol. **16**, 1209–1217 (2019)

72. I.R. Agool, K.J. Kadhim, A. Hashim, Fabrication of new nanocomposites: (PVA-PEG-PVP) blend-zirconium oxide nanoparticles) for humidity sensors. Int. J. Plast. Technol. **21**, 397–403 (2017)

73. F.H. Abd El-Kader, S.A. Gafer, A.F. Basha, S.I. Bannan, M.A.F. Basha, Thermal and optical properties of gelatin/poly(vinylalcohol) blends. J. Appl. Polym. Sci. **118**, 413–420 (2010)

74. S.H. Wemple, M. Di Domenico Jr., Behavior of the electronic dielectric constant in covalent and ionic materials. Phys. Rev. B **4**, 1138–1151 (1971)

75. E. Marquez, P. Nagels, J.M. Gonzalez-Leal, A.M. Bernal-Otiva, E. Sleeckx, R. Callaerts, Vacuum **52**, 55–60 (1999)

76. A.H. Ammar, A.M. Farid, M.A.M. Seyam, Heat treatment effect on the structural and optical properties of $AgInSe_2$ thin films. Vacuum **66**, 27–38 (2002)

77. A.H. Ammar, Studies on some structural and optical properties of $Zn_xCd_{1-x}Te$ thin films. Appl. Surf. Sci. **201**, 9–19 (2002)

78. K. Tanaka, Optical properties and photo induced changes in amorphous As-S films. Thin Solid Films **66**, 271–279 (1980)

79. S.H. Wemple, Ionicity, valency, and band inversion in $Pb_{1-x}Sn_xTe$. Phys. Lett. **45A**(5), 401–403 (1973)

80. B.M. Baraker, B. Lobo, Dispersion parameters of cadmium chloride doped PVA-PVP blend films. J. Polym. Res. **24**, 84 (2017)

81. A.F. Mansour, A. Elfalaky, F.A. Maged, Synthesis, characterization and optical properties of PANI/PVA blends. IOSR J. Appl. Phys. **7**(4), 37–45 (2015)

82. C.H. Kittel, *Introduction to Solid State Physics*, 6th edn. (Wiley, Hoboken, 1986)

83. M. Caglar, M. Zor, S. Ilican, Y. Caglar, Effect of indium incorporation on the optical properties of spray pyrolyzed $Cd_{0.22}Zn_{0.7}8S$ thin films. J. Phys. **56**(3), 277–287 (2006)

84. O.G. Abdullah, S.B. Aziz, K.M. Omer, Y.M. Salih, Reducing the optical band gap of polyvinyl alcohol (PVA) based nanocomposite. J. Mater. Sci. **26**(7), 5303–5309 (2015)

85. R.R. Karria, M. Tanzifi, M.T. Yarakic, J.N. Sahu, Optimization and modeling of methyl orange adsorption onto polyaniline nano-adsorbent through response surface methodology and differential evolution embedded neural network. J. Environ. Manag. **223**, 517–529 (2018)

86. Z. Wu, L. Li, Y. Mu, X. Wan, Synthesis and adhesive property study of a mussel-inspired adhesive based on poly(vinyl alcohol) backbone. Macromol. Chem. Phys. **218**(16), 1–9 (2017)

87. Q. Bai, G. Zhang, B. Xu, X. Feng, H. Jiang, H. Li, Thermal and water dual-responsive shape memory poly(vinyl alcohol)/Al_2O_3 nanocomposite. RSC Adv. **5**(111), 91213–91217 (2015)